Development/Plasticity/Repair

Chondroitinase ABC Promotes Sprouting of Intact and Injured Spinal Systems after Spinal Cord Injury

A. W. Barritt,* M. Davies,* F. Marchand, R. Hartley, J. Grist, P. Yip, S. B. McMahon, and E. J. Bradbury
Neurorestoration Group, Wolfson Centre for Age Related Diseases, King's College London, London SE1 1UL, United Kingdom

Chondroitin sulfate proteoglycans (CSPGs) are inhibitory extracellular matrix molecules that are upregulated after CNS injury. Degradation of CSPGs using the enzyme chondroitinase ABC (ChABC) can promote functional recovery after spinal cord injury. However, the mechanisms underlying this recovery are not clear. Here we investigated the effects of ChABC treatment on promoting plasticity within the spinal cord. We found robust sprouting of both injured (corticospinal) and intact (serotonergic) descending projections as well as uninjured primary afferents after a cervical dorsal column injury and ChABC treatment. Sprouting fibers were observed in aberrant locations in degenerating white matter proximal to the injury in regions where CSPGs had been degraded. Corticospinal and serotonergic sprouting fibers were also observed in spinal gray matter at and below the level of the lesion, indicating increased innervation in the terminal regions of descending projections important for locomotion. Spinal-injured animals treated with a vehicle solution showed no significant sprouting. Interestingly, ChABC treatment in uninjured animals did not induce sprouting in any system. Thus, both denervation and CSPG degradation were required to promote sprouting within the spinal cord. We also examined potential detrimental effects of ChABC-induced plasticity. However, although primary afferent sprouting was observed after lumbar dorsal column lesions and ChABC treatment, there was no increased connectivity of nociceptive neurons or development of mechanical allodynia or thermal hyperalgesia. Thus, CSPG digestion promotes robust sprouting of spinal projections in degenerating and denervated areas of the spinal cord; compensatory sprouting of descending systems could be a key mechanism underlying functional recovery.

Key words: **proteoglycan; plasticity; spinal cord; regeneration; denervation; repair**

Introduction

Many factors contribute to the lack of repair after spinal cord injury (SCI), including a lack of growth-promoting factors (Widenfalk et al., 2001), poor intrinsic regenerative capacity of CNS neurons (Neumann and Woolf, 1999), inhibitory factors associated with CNS myelin (Filbin, 2003; McGee and Strittmatter, 2003; Schwab, 2004), chemorepulsive molecules (De Winter et al., 2002), and glial scar-associated inhibitors such as chondroitin sulfate proteoglycans (CSPGs) (Silver and Miller, 2004; Carulli et al., 2005).

CSPGs are extracellular matrix molecules that are upregulated around CNS injury sites (Asher et al., 2000, 2002; Jones et al., 2003; Tang et al., 2003) and inhibit neurite outgrowth *in vitro* (Snow et al., 1990; Smith-Thomas et al., 1994, 1995; Dou and Levine, 1994, 1997) and *in vivo* (Davies et al., 1997, 1999). Degradation of the glycosaminoglycan (GAG) component of CSPG molecules using chondroitinase ABC (ChABC) renders inhibitory substrates more permissive to growth (McKeon et al., 1995; Zuo et al., 1998; Yu and Bellamkonda, 2001; Grimpe et al., 2005) and enhances axon regeneration after CNS injury (Moon et al., 2001; Bradbury et al., 2002; Yick et al., 2003, 2004; Chau et al., 2004; Fouad et al., 2005; Ikegami et al., 2005; Houle et al., 2006).

More importantly, beneficial effects on functional recovery after ChABC treatment have now been demonstrated in a number of SCI models, including dorsal column injury (Bradbury et al., 2002), contusion (Caggiano et al., 2005), hemisection (Yick et al., 2004; Houle et al., 2006), and transection (Fouad et al., 2005). However, the mechanisms underlying this recovery are not clear. The degree of axonal regeneration observed by us (Bradbury et al., 2002) and others has been modest at best, suggesting that other mechanisms contribute to functional restoration, such as plasticity of other systems (Bradbury and McMahon, 2006). There is evidence that manipulating CSPGs using ChABC induces plasticity in the adult brain (Pizzorusso et al., 2002; Tropea et al., 2003; Rhodes and Fawcett, 2004; Corvetti and Rossi, 2005) and promotes sprouting of sensory projections terminating within the brainstem (Massey et al., 2006). However, the effects of CSPG degradation on plasticity within the spinal cord have not been investigated, particularly in descending systems important for motor function. Also, whether ChABC-mediated plasticity can occur in the absence of an injury has not been determined.

Here we examine the response of intact (serotonergic and primary afferent) and injured (corticospinal) systems after cervical SCI and ChABC treatment in adult rats, using the same model that first demonstrated beneficial effects of ChABC on functional

Received March 1, 2006; revised Aug. 29, 2006; accepted Sept. 5, 2006.

This work was supported by the United Kingdom Medical Research Council. We thank Sonia Akrimi, Jodie Hall, Marta Agudo, Sophie Pezet, Jonathan Ramsey, and Viv Cheah for expert assistance and Tim Boucher and Dave Bennett for critical review of this manuscript.

*A.W.B. and M.D. contributed equally to this work.

Correspondence should be addressed to Dr. Elizabeth J. Bradbury, Neurorestoration Group, Wolfson Centre for Age Related Diseases, King's College London, Wolfson Wing, Hodgkin Building, Guy's Campus, London Bridge, London SE1 1UL, UK. E-mail: elizabeth.bradbury@kcl.ac.uk.

DOI:10.1523/JNEUROSCI.2980-06.2006

 0270-6474/06/2610856-12$15.00/0

recovery (Bradbury et al., 2002). We find that ChABC induces *de novo* sprouting in degenerating white-matter tracts close to the SCI in areas of CSPG degradation as well as increased innervation of denervated gray matter caudal to the SCI. We also determined the effects of ChABC treatment on pain sensitivity and did not observe reduced pain thresholds or increased connectivity of nociceptive neurons. This is the first demonstration that ChABC can induce plasticity of injured and intact projections within the spinal cord after SCI and offers a mechanism for its potent effects on functional recovery.

Materials and Methods

Animals

A total of 82 adult male Wistar rats (220–250 g; Banton and Kingman, Hull, UK) were used in these studies. For cervical sprouting studies, rats received a cervical SCI plus treatment with either ChABC ($n = 16$) or a vehicle control solution ($n = 16$). Control (uninjured) animals were treated with ChABC ($n = 16$) or were untreated ($n = 16$). For pain studies, animals received a lumbar SCI plus treatment with either ChABC ($n = 6$) or a vehicle control solution ($n = 6$), and a control (uninjured) group had sham surgery ($n = 6$). All surgical procedures were performed in accordance with United Kingdom Home Office regulations.

Cervical SCI and ChABC treatment

Surgical procedures were performed under anesthesia using a mixture of intraperitoneal medetomidine (0.25 mg/kg) and ketamine (60 mg/kg), and sterile precautions were used throughout. In the first series of experiments, the lesion was performed in the cervical spinal cord where the dorsal columns were crushed at spinal level C4 (Bradbury et al., 2002). Briefly, a partial laminectomy was performed, and lignocaine (2%; Antigen Pharmaceuticals, Roscrea, Ireland) was applied to the spinal cord. A small slit was made in the dura, and the dorsal columns were crushed with fine watchmakers forceps (0.3 mm tips). The forceps were positioned on either side of the dorsal columns, pushed 2 mm down into the cord, and held tightly together for 10 s before raising them back out of the cord. A flexible silastic catheter (external diameter, 1.14 mm; Merck, Essex, UK) was inserted subdurally for delivery of bolus intrathecal injections of ChABC (Bradbury et al., 2002). The tubing was inserted via the atlanto-occipital membrane and pushed 8 mm to lie rostral to the lesion site. The tubing was secured to the atlanto-occipital bone with cyanoacrylate, and the external end was guided under the skin and externalized over the head. Rats received bolus injections of protease-free ChABC (10 U/ml, 6 μl; Seikagaku Corporation, Tokyo, Japan) via the externalized catheter using a Hamilton syringe, followed by a saline flush (6 μl). ChABC was delivered for the first 10 d after SCI, with the first injection immediately after injury and subsequent injections on days 2, 4, 6, 8, and 10 (performed under inhalation anesthesia, 2% isofluorane in O_2). Vehicle-treated rats underwent identical procedures but received injections of saline (6 μl followed by 6 μl). Two control groups received sham surgery whereby the surgical procedures were followed until exposure of the spinal cord but no lesion was made; one of these groups received injections of ChABC (as above), and the other was untreated. Animals were killed 4 weeks after injury for anatomical assessments of plasticity ($n = 8$ per group for assessment of corticospinal tract (CST) and serotonergic and primary afferent plasticity using immunocytochemical methods; $n = 4$ per group for assessment of CST axon tracing) or 11 d after injury for anatomical assessments of CSPG degradation ($n = 4$ per group).

Anterograde tracing of CST axons

One week after SCI surgery, rats were reanesthetized (as above) and positioned in a stereotaxic frame. Biotinylated dextran amine (BDA; 10,000 MW; Invitrogen, Eugene, OR) was injected into the sensorimotor cortex at six sites bilaterally using the following coordinates (in reference to bregma): (1) 2.5 mm lateral and 1.5 mm posterior; (2) 3.5 mm lateral and 0.5 mm posterior; (3) 3.5 mm lateral and 0.5 mm anterior; (4) 1.5 mm lateral and 1.0 mm anterior; (5) 2.5 mm lateral and 1.5 mm anterior; and (6) 3.5 mm lateral and 2.0 mm anterior (Neafsey et al., 1986). Injections were made 2 mm from the surface of the cortex, and 0.5 μl of BDA (10% w/v in sterile PBS) was injected into each site via a G26 needle attached to a micro-infusion pump (delivered at a rate of 0.25 μl/min and left for an additional 1 min before withdrawal). Three weeks later, animals were anesthetized and perfused transcardially (see below).

Lumbar SCI and ChABC treatment

In the second series of experiments, we assessed whether increased primary afferent sprouting could lead to increased pain sensitivity. These experiments were performed in the lumbar spinal cord because thermal hyperalgesia and mechanical allodynia are classically assessed in the hindpaw. The dorsal columns were lesioned as above, but at spinal level L2. For delivery of ChABC, a small laminectomy was performed at T9, and silastic tubing was inserted via a small slit in the dura and pushed 10 mm to lie rostral to the lesion site. The tubing was secured to a rostral vertebral bone with cyanoacrylate and externalized as above. For ChABC-treated rats ($n = 6$), bolus injections of ChABC were delivered as above with the same dose, volume, and treatment days but with a greater volume of saline flush (10 μl) because of the longer catheter required. Vehicle-treated rats ($n = 6$) underwent identical procedures but received injections of saline (6 μl followed by 10 μl). An additional control group ($n = 6$) received sham surgery whereby the surgical procedure was followed until exposure of the spinal cord but no lesion was made. Animals were killed 5 weeks after injury (after behavioral testing and cFos induction) for anatomical assessment of primary afferent sprouting and functional connectivity.

Behavioral testing

In lumbar spinal-injured rats, preoperative and postoperative mechanical and thermal thresholds were ascertained to assess the effects of SCI and treatment with ChABC on pain sensitivity. The experimenter was blind to treatment groups throughout the testing period. Noxious thermal sensitivity was assessed using the method of Hargreaves et al. (1988), by measuring the time taken for a radiant heat source to elicit a flexion reflex. Each paw was tested three times (and averaged to obtain the mean withdrawal latency). Mechanical withdrawal thresholds were tested using a Dynamic Plantar Aesthesiometer (Ugo Basile, Milan, Italy), in which a mechanical stimulus was applied via an actuator filament (0.5 mm diameter), which under computer control applies a linear ramp of 2.5 g/s to the plantar surface of the paw. The withdrawal threshold was calculated as the average of three consecutive tests. Presurgery baselines were recorded, and postlesion testing was performed on days 3, 7, 14, 21, and 28 after injury. Statistical analysis of behavioral data were performed using SigmaStat (SPSS, Chicago, IL) software (two-way repeated-measures ANOVA comparing groups vs days).

*Induction of c-*fos

After the completion of behavioral testing, animals were left for 1 week, and the functional connectivity of primary afferents was determined by assessing the expression of the immediate-early gene c-*fos* after a noxious heat stimulus. Under terminal urethane anesthesia (1.5 g/kg, i.p.), the left hindpaw was immersed up to the ankle in a 52°C water bath for 30 s. After 2 h, rats were perfused, and lumbar spinal cord tissue was processed for the expression of cFos protein in spinal dorsal horn neurons (see below).

Tissue processing

Rats were deeply anesthetized with pentobarbitone (80 mg/kg, i.p.) and perfused with 100 ml of heparinized saline, followed by 300 ml of paraformaldehyde (4% in 0.1 M phosphate buffer; for c-*fos* experiments, 15% picric acid was added to the fixative). Blocks of spinal cord tissue containing the lesion site plus 10 mm rostral and 10 mm caudal were dissected, and tissue was postfixed for 2 h (at 4°C). For plasticity studies in the cervical cord, tissue was transferred to PBS (plus 0.1% sodium azide) and embedded in gelatin (10%, 300 bloom; Sigma, Poole, UK). Gelatin blocks were hardened in 4% paraformaldehyde, and 40 μm free-floating serial transverse sections were cut on a vibratome (Leica, Nussloch, Germany) and collected in 24-well plates containing PBS (plus 0.1% sodium azide). For studies in the lumbar cord, tissue was transferred to 20% sucrose in 0.1 M phosphate buffer (three nights at 4°C) and frozen in OCT embedding compound (BDH, Essex, UK). Transverse sections (20 μm) through the lumbar spinal cord (L3–L6) were cryostat cut, and sections

were collected free floating into 24-well plates containing PBS (plus 0.1% sodium azide).

Immunohistochemistry

Protein kinase C-γ, calcitonin gene-related peptide, and serotonin. For visualization of fiber sprouting at different levels rostral, ventral, and caudal to an SCI, free-floating spinal cord sections were washed in PBS and incubated overnight at 20°C with the following antibodies (diluted in PBS plus 0.2% Triton X-100): rabbit anti-protein kinase C-γ (PKCγ) (1:500; Santa Cruz Biotechnology, Santa Cruz, CA), rabbit anti-calcitonin gene-related peptide (CGRP; 1:4000; Sigma), and rabbit anti-serotonin (1:16,000; DiaSorin, Stillwater, MN). After three washes in PBS, sections were then incubated with donkey anti-rabbit tetramethylrhodamine isothiocyanate-conjugated antibody (1:200, 4 h at 20°C; Jackson ImmunoResearch, West Grove, PA). Sections were slide mounted and coverslipped with Vectashield mounting medium (Vector Laboratories, Burlingame, CA).

Chondroitin-4-sulfate. For visualization of CSPG GAG digestion, sections were processed for chondroitin-4-sulfate (C-4-S) immunostaining to reveal digested sugar stub regions. Free-floating cervical and lumbar spinal cord sections were incubated in the following (with three PBS washes between each step): hydrogen peroxide (0.3%, 20 min), mouse monoclonal anti-C-4-S (1:5000, overnight at 20°C; ICN Biochemicals, Aurora, OH), biotinylated horse anti-mouse secondary antibody (1:400, 90 min; Jackson ImmunoResearch, West Grove, PA), ABC reagent (1:250, 30 min; Vector Laboratories), biotinyl tyramide (1:75, 10 min; PerkinElmer Life Sciences, Boston, MA), and extra-avidin FITC (1:500, 2 h; Sigma). Sections were slide mounted and coverslipped as above. For colocalization studies (C-4-S and CGRP), the C-4-S immunostaining was always performed first (as above), followed by CGRP immunostaining (as above).

BDA. Every third section through C2–C6 was processed for BDA labeling to obtain a rostrocaudal serial reconstruction of CST fiber sprouting. Free-floating sections were incubated in the following (with three PBS washes between each step): biotinylated horse anti-mouse secondary antibody (1:400, 90 min; Jackson ImmunoResearch), ABC reagent (1:250, 30 min; Vector Laboratories), biotinyl tyramide (1:75, 10 min; PerkinElmer Life Sciences), and extra-avidin FITC (1:500, 2 h; Sigma). Sections were slide mounted and coverslipped as above.

c-fos. For visualization of functional connectivity of sprouting primary afferents, free-floating lumbar spinal cord sections were incubated in the following (with three PBS washes between each step): H_2O_2 (0.3%, 10 min), rabbit anti-c-*fos* (1:2500, overnight; Calbiochem, La Jolla, CA), biotinylated donkey anti-rabbit secondary antibody (1:300, 1 h; Jackson ImmunoResearch), ABC reagent (1:500, 1 h; Vector Laboratories), biotinyl tyramide (1:75, 10 min; PerkinElmer Life Sciences), and extra-avidin FITC (1:500, 2 h; Sigma). Sections were slide mounted and coverslipped as above.

Quantification of sprouting.

In all cases, quantification was performed with the experimenter blind to the treatment group.

PKCγ. Four transverse sections per animal at spinal levels C2 and C3 were selected for analysis. KS 300 software (Vision; Zeiss, Oberkochen, Germany) was used to determine relative intensity of PKCγ immunofluorescence within three defined regions of the dorsal columns (using three boxes positioned along a dorsoventral axis) (see Fig. 1*B*). The gross intensity values obtained for each region were then averaged. A reference intensity of unstained tissue was also measured by a fourth box on all sections. Background intensity was deducted from the average gross intensity to calculate the mean net PKCγ staining intensity.

BDA. Two transverse sections per animal at each of five spinal levels (C2–C6) were selected for analysis. Relative intensity of BDA labeling was determined within a defined region of spinal gray matter using the method described above (with a box positioned in the intermediate gray matter) (see Fig. 2*A*). Pixel threshold analysis was also performed in the same tissue using SigmaScan software. The thresholds for positive staining were set, and the number of pixels above threshold was calculated.

Serotonin. Four transverse sections per animal at level C4 (lesion epicenter) and level C6 (caudal to the lesion) were selected for analysis. Relative intensity of serotonin immunofluorescence was determined within two defined regions using the method described above (with one box positioned in the ventral white matter at C4 and the other in the ventral horn at C6) (see Fig. 4*A*). Pixel threshold analysis was also performed in the C6 ventral horn region (method as above).

CGRP. Four transverse sections per animal at spinal level C5 were selected for analysis. Relative intensity of CGRP immunofluorescence was determined within four defined regions of the dorsal columns using the method described above. Three of the intensity measurement boxes were positioned in the superficial white matter dorsal to the dorsal horn, and one was positioned in the gracile fasciculus (see Fig. 5*A*).

c-fos. Four transverse sections per rat at each of the spinal levels L3–L6 were selected for analysis. The number of *c-fos*-immunoreactive nuclei within the superficial dorsal horn was counted, and an average of the number of nuclei per section was calculated for each animal.

Statistical analyses of intensity measurements, cell counts, and pixel number were performed using SPSS software: one-way ANOVA comparing groups for PKCγ, serotonin, CGRP, and cFos; two-way ANOVA comparing groups and spinal levels for BDA analysis.

Results

ChABC promotes sprouting of the CST rostral, within, and caudal to an SCI

PKCγ immunocytochemistry

PKCγ immunostaining in spinal segments C2 and C3 revealed a normal expression pattern in control (uninjured) animals, being present in the main dorsal CST projecting in the ventral portion of the dorsal columns and in interneurons in the superficial dorsal horn (Fig. 1*A*,*B*). A similar pattern of staining was seen in uninjured animals treated with ChABC (Fig. 1*C*,*D*). Four weeks after a C4 dorsal column lesion and vehicle treatment, PKCγ immunoreactivity in the CST was markedly reduced in the two spinal segments (C2–C3) above the injury (Fig. 1*E*,*F*), indicative of CST die-back. After a C4 dorsal column lesion and ChABC treatment, PKCγ immunoreactivity in the main CST projection was also reduced in the two spinal segments above the injury, although to a lesser extent than that of lesioned animals treated with vehicle (Fig. 1*G*,*H*); however, in these animals, PKCγ immunoreactivity was also observed in the dorsal portion of the dorsal columns, where the CST does not normally project (Fig. 1*G*,*H*). Quantification of PKCγ immunoreactivity in the dorsal columns at levels C2 and C3 confirmed the presence of enhanced PKCγ immunoreactivity in aberrant areas of the dorsal columns after injury and treatment with ChABC (Fig. 1*I*,*J*). Lesioned animals treated with either vehicle or ChABC had significantly reduced intensity of PKCγ immunoreactivity in the ventral portion of the dorsal columns compared with unlesioned controls (both naive and ChABC treated) ($p < 0.05$, one-way ANOVA, Holm-Sidak *post hoc*), whereas in the medial and dorsal portions of the dorsal columns, lesioned animals treated with ChABC, but not vehicle, had significantly increased intensity of PKCγ immunoreactivity compared with unlesioned controls ($p < 0.05$, one-way ANOVA, Holm-Sidak *post hoc*) (Fig. 1*I*). Statistical comparisons of ChABC treatment compared with vehicle treatment after lesion revealed significant differences in the dorsal portion of the dorsal columns at C2 and in both medial and dorsal portions at C3 ($p < 0.05$, one-way ANOVA, Holm-Sidak *post hoc*). Thus, treatment with ChABC induces CST sprouting rostral to an SCI in the dorsal aspect of the dorsal columns, a region that contains degenerating ascending projections.

BDA labeling

The PKCγ antibody used here gives a diffuse label of the CST projection and is therefore a convenient marker for bulk labeling

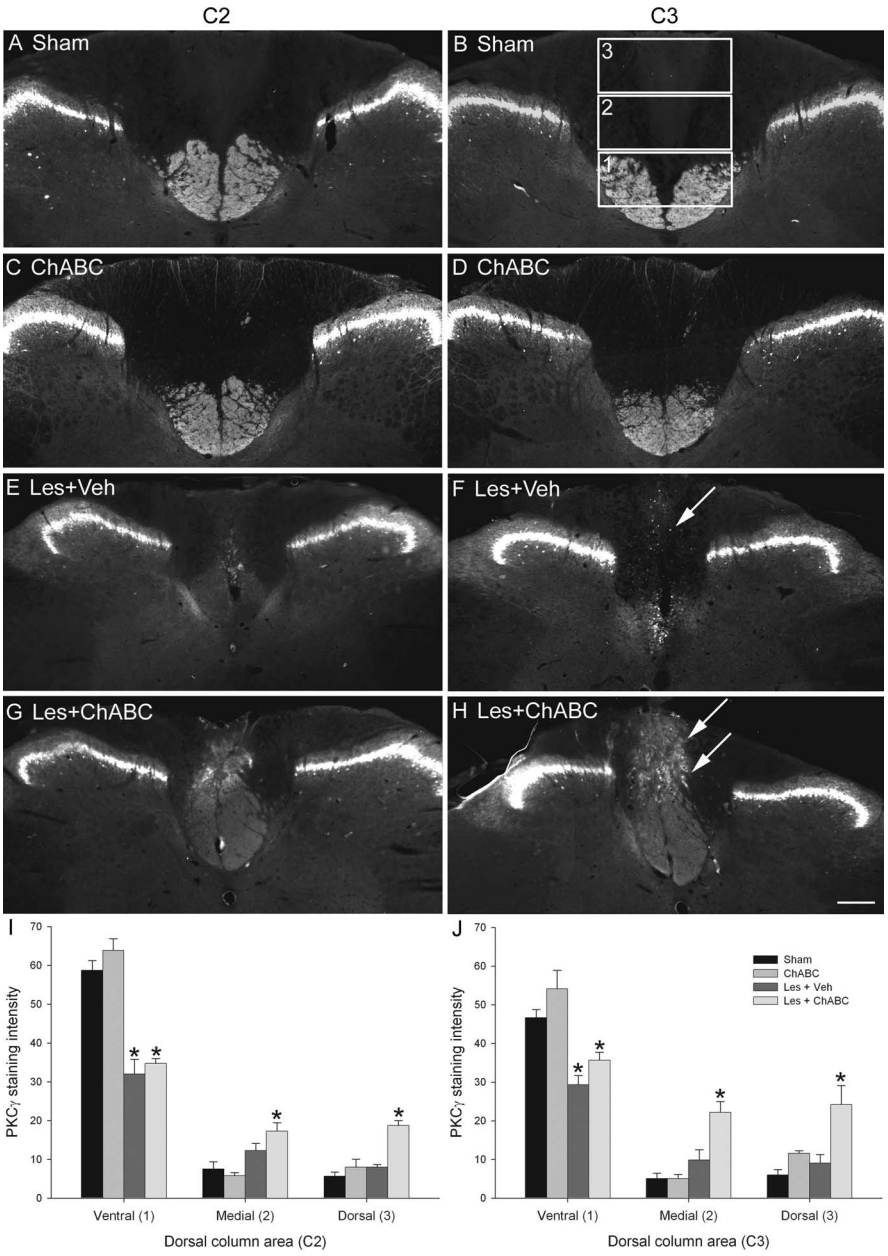

Figure 1. ChABC promotes plasticity of the CST rostral to a C4 dorsal column lesion. ***A–H***, PKCγ immunostaining in transverse sections of the cervical spinal cord at spinal levels C2 (***A***, ***C***, ***E***, ***G***) and C3 (***B***, ***D***, ***F***, ***H***) reveals the normal projection of the CST in the ventral part of the dorsal columns in sham (unlesioned) animals (***A***, ***B***) and ChABC-treated unlesioned animals (***C***, ***D***). Four weeks after a C4 dorsal column lesion, the CST was mostly absent in the two segments above the injury level after vehicle control treatment (***E***, ***F***), indicating significant die-back of this tract after injury. CST die-back rostral to injury was also apparent in lesioned animals treated with ChABC; however, in these animals, the CST was observed sprouting into the denervated dorsalmost parts of the dorsal columns, where the ascending projection normally runs (***G***, ***H***). Arrows indicate the lack of CST growth after lesion and vehicle treatment (***F***) compared with the robust CST sprouting after lesion and ChABC treatment (***H***) at the C3 level. Boxed areas in ***B*** denote regions selected for quantification. Scale bar, 200 μm. ***I***, ***J***, Quantification in three defined regions at levels C2 (***I***) and C3 (***J***) confirmed a significant reduction in PKCγ in the ventral portion of the dorsal columns after injury and *de novo* expression of PKCγ in the medial and dorsal portions of the dorsal columns after ChABC, but not vehicle, treatment. The asterisks denote a significant difference from sham controls. Error bars indicate SEM. Veh, Vehicle; Les, lesion.

of the tract to determine where it projects in the dorsal columns. It does not, however, label CST terminals (Mori et al., 1990). Therefore, to determine whether sprouting CST fibers innervate spinal cord gray matter, we also analyzed anterogradely labeled CST axons. BDA tracing in control animals revealed punctate labeling of the CST projection in the dorsal columns and numerous fibers innervating the spinal cord gray matter, with similar labeling and termination patterns observed in both naive and ChABC-treated uninjured animals (Fig. 2*A*,*B*). Serial reconstruction from C2–C6 revealed that after a C4 dorsal column lesion and vehicle treatment, the CST projection in the dorsal columns appeared reduced in spinal segments C2 and C3 and there was also a marked reduction in fibers innervating spinal gray matter, although some innervation was still apparent in areas directly adjacent to the dorsal columns (Figs. 2*C*,*E*, 3*A*,*C*). In contrast, after C4 dorsal column lesion and treatment with ChABC, numerous sprouting fibers were observed in the dorsal columns, with intense bundles of fibers apparent, both within the appropriate ventral portion as well as sprouting up into dorsal regions of the dorsal columns (Fig. 2*D*,*F*), confirming the findings observed with PKCγ. Furthermore, numerous fibers were observed innervating spinal gray matter, apparent directly adjacent to the dorsal columns, in the dorsal horns, and extending ventrolaterally in the intermediate gray matter (Figs. 2*D*,*F*, 3*B*,*D*). At the lesion epicenter (C4), differences in CST innervation of spinal gray matter between lesioned animals treated with vehicle or ChABC were even more striking (Fig. 2, compare *G*, *H*). In vehicle-treated animals, some CST fibers were apparent in gray matter adjacent to the lesioned dorsal columns, although these were relatively sparse (Figs. 2*G*, 3*E*). However, in ChABC-treated animals, extensive arborization within spinal gray matter was observed, with numerous fibers apparent in dorsal and intermediate gray matter, despite a complete absence of the CST in the lesioned dorsal columns, indicating robust sprouting and regenerative growth (Figs. 2*H*, 3*F*). In sections caudal to the injury (C5 and C6), virtually no labeled fibers were observed in lesioned animals treated with vehicle (Figs. 2*I*,*J*, 3*G*,*I*), whereas numerous fibers were still apparent at C5 in ChABC-treated animals, with a smaller number still apparent at level C6 (Figs. 2*K*,*L*, 3*H*,*J*), indicating frank regeneration of CST axons caudal to the SCI. Quantification of CST sprouting in the spinal gray matter of lesioned animals was first determined by analyzing the staining intensity of BDA-labeled fibers in a defined region of spinal gray matter at spinal levels C2–C6. This confirmed a significant increase in staining intensities after ChABC treatment compared with vehicle at levels C3–C5 ($p < 0.05$, two-way ANOVA, Student–Neumann–Keuls *post hoc* tests) (Fig. 3*K*). To determine whether increased intensity measurements were attributable to an increased number of fibers, we also determined

the mean pixel counts above a threshold intensity and found the number of positive pixels to be significantly increased at levels C3–C5 ($p < 0.05$, two-way ANOVA, Student–Neumann–Keuls *post hoc* tests) (Fig. 3*L*), confirming that the significant increase in BDA-labeling intensity did indeed signify new fiber growth. Thus, ChABC treatment promotes robust sprouting of CST fibers rostral, within, and caudal to a dorsal column injury.

ChABC promotes sprouting of serotonergic fibers ventral and caudal to an SCI

Although we have demonstrated that ChABC can induce *de novo* growth of the CST after SCI, it is unclear whether the aberrant CST fibers are sprouting or regenerating because the CST was lesioned. Therefore, we also investigated plasticity of an intact descending system after injury and ChABC treatment by assessing plasticity of the serotonergic pathway. Serotonin immunostaining in the cervical cord revealed a normal expression pattern in control (uninjured) animals, with serotonin-immunoreactive fibers present predominantly in the superficial dorsal horn, lamina X, and the ventral horn, with very little immunoreactivity observed in spinal white matter (Fig. 4*A*). A similar pattern of staining was seen in uninjured animals treated with ChABC (Fig. 4*B*). Four weeks after a C4 dorsal column lesion and vehicle treatment, some sprouting of serotonergic immunoreactive fibers was observed rostral to the lesion site, as has been reported previously (Bruce et al., 2002), and some fibers were also evident ventral to the lesion at the level of the lesion epicenter (C4) (Fig. 4*C*). However, after dorsal column lesion and treatment with ChABC, as well as some sprouting being apparent around the lesion cavity, robust sprouting also occurred ventral to the injury site, with intense immunoreactivity and numerous sprouting fibers apparent in the ventral columns (Fig. 4*D*). Sprouting in the ventral white matter was only observed within spinal segment C4 (i.e., in degenerating areas close to the injury). To determine whether increased sprouting in the ventral white matter, where these descending axons project (Schmidt and Jordan, 2000), leads to increased innervation of the gray matter, we also examined serotonin expression in the ventral horn caudal to the lesion site. At spinal level C6, levels of serotonin immunoreactivity were similar in uninjured control animals (both naive and ChABC treated) and in vehicle-treated lesioned animals (Fig. 4*E–G*, respectively). However, there was a marked increase in serotonin immunoreactivity within the ventral horn of lesioned animals after ChABC treatment, with intense immunoreactivity indicating dense innervation (Fig. 4*H*). Quantification of serotonergic fiber sprouting in the ventral white matter at C4 and ventral horn at C6 confirmed the presence of enhanced serotonergic immunoreactivity after injury and treatment with ChABC (Fig. 4*I*). Although there was a trend for an increase in serotonin in the ventral white matter of lesioned animals treated with vehicle, this did not reach significance, with intensity measurements in both the ventral white matter and caudal ventral horn not significantly different from those of unlesioned controls (both naive and ChABC treated) ($p > 0.05$, one-way ANOVA, Holm-Sidak *post hoc*). However, lesioned animals treated with ChABC had signif-

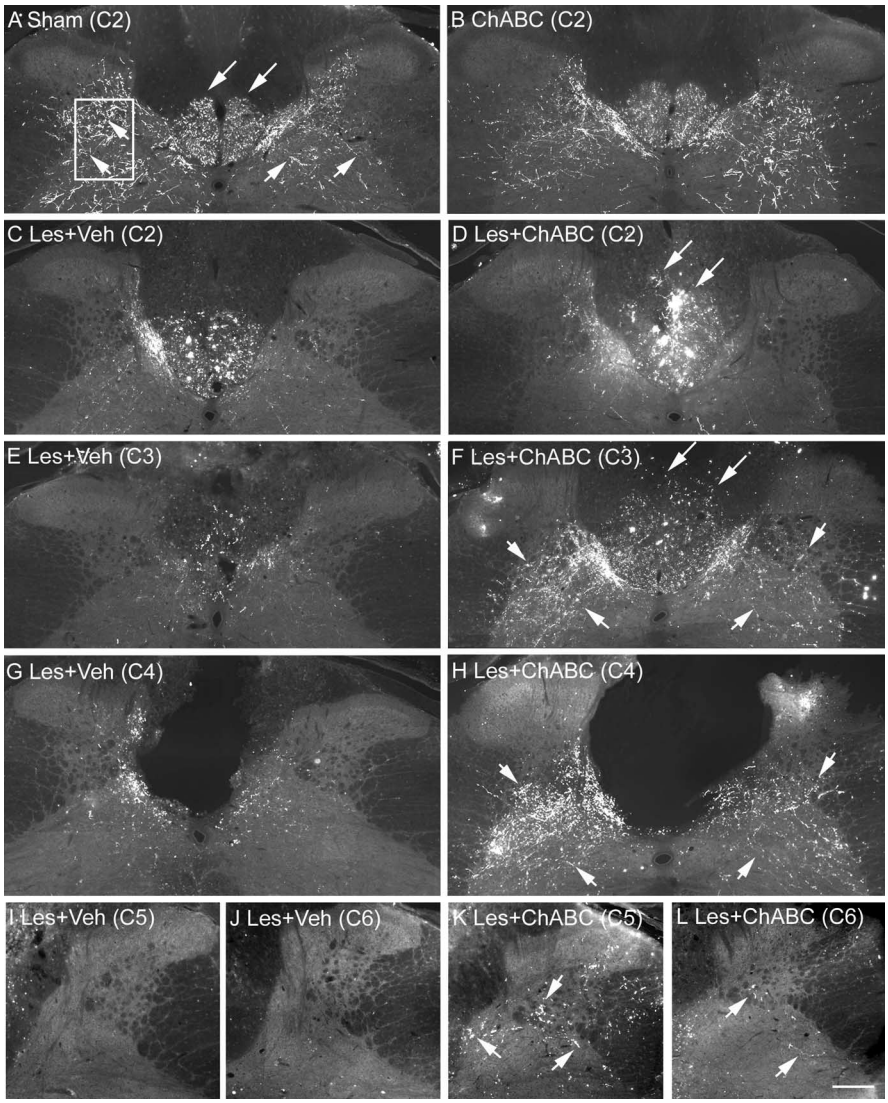

Figure 2. ChABC promotes plasticity of CST fibers rostral, within, and caudal to a C4 dorsal column lesion. ***A***, BDA tracing in transverse sections of the cervical spinal cord in sham (uninjured) controls reveals punctate labeling of the CST projection in the ventral portion of the dorsal columns (long arrows) and numerous collaterals innervating spinal gray matter (short arrows). The boxed area denotes the area selected for quantification of CST sprouting in gray matter (see Fig. 3). ***B***, A similar pattern is observed in uninjured animals treated with ChABC. ***C***, ***E***, Serial reconstruction from C2–C6 in lesioned animals treated with vehicle reveals die-back of the CST projection in the dorsal columns as well as decreased innervation of gray matter rostral to the injury at levels C2 and C3. ***D***, ***F***, In contrast, after ChABC treatment, there is reduced CST die-back, numerous intensely labeled bundles of CST axons sprouting dorsally in the dorsal columns (long arrows), and increased CST fibers innervating spinal gray matter (short arrows) rostral to the injury. ***G***, ***H***, At the lesion epicenter (C4), the difference in fiber sprouting within spinal gray matter is compelling with sparse innervation after vehicle treatment (***G***) and abundant innervation after ChABC treatment, despite a complete absence of the CST (***H***). ***I***, ***J***, Caudal to the lesion, few, if any, CST fibers were observed in gray matter after vehicle treatment. ***K***, ***L***, However, after ChABC treatment, numerous fibers were observed at level C5 (***K***) and a small number of fibers were still apparent at C6 (***L***). Scale bar, 200 μm. Veh, Vehicle; Les, lesion.

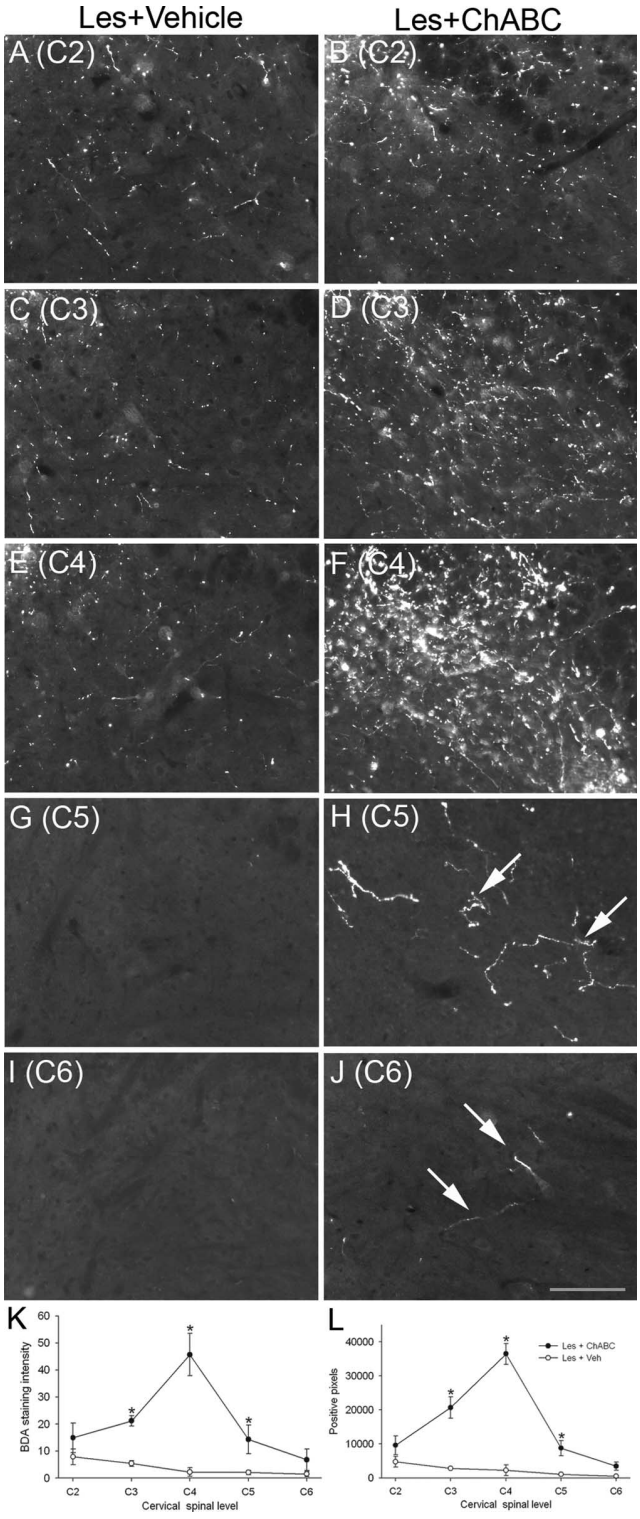

Figure 3. ChABC promotes plasticity of CST fibers rostral, within, and caudal to a C4 dorsal column lesion. ***A–J***, High-power images of BDA labeling in the spinal gray matter of lesioned animals treated with vehicle (***A***, ***C***, ***E***, ***G***, ***I***) or ChABC (***B***, ***D***, ***F***, ***H***, ***J***) showing representative examples of CST fiber sprouting at spinal levels C2–C6. Decreased innervation was apparent rostral to the C4 injury, and no fibers were observed in caudal levels after vehicle treatment; in contrast robust, CST sprouting was apparent rostral to and at the level of the C4 lesion site and regenerating fibers were observed in caudal levels after ChABC treatment. ***K***, ***L***, Quantification of both BDA staining intensity (***K***) and the number of positive pixels above a threshold (***L***) revealed a significant increase in CST fibers innervating spinal gray matter after ChABC treatment compared with vehicle treatment, with maximal sprouting occurring at the lesion epicenter (C4) and significant sprouting at both rostral and caudal spinal levels. Asterisks denote a significant difference from sham controls. Scale bar, 200 μm. Les, Lesion; Veh, vehicle. Error bars indicate SEM.

icantly increased intensity of serotonergic immunoreactivity compared with unlesioned controls in both areas ($p < 0.05$, one-way ANOVA, Holm-Sidak *post hoc*). Statistical comparisons of ChABC treatment compared with vehicle treatment after lesion also revealed a significant difference in both areas ($p < 0.05$, one-way ANOVA, Holm-Sidak *post hoc*). To determine whether the increased intensity measurements within the ventral horn were as a result of increased serotonin expression in fibers already present or an increased number of fibers, we also performed a threshold pixel analysis. The mean pixel count ± SEM (of a 1.3 million pixel sample) above a threshold intensity was significantly higher in lesioned animals treated with ChABC (115,482 ± 26,412) compared with lesioned animals treated with vehicle (33,021 ± 11,612; $p < 0.05$, *t* test), confirming that the significant increase in serotonin intensity did indeed signify new fiber growth. Thus, treatment with ChABC induces plasticity of descending serotonergic fibers at the level of an SCI, in a region that is undergoing secondary degeneration and in denervated gray matter caudal to the injury.

ChABC promotes sprouting of intact primary afferents caudal to an SCI

To investigate plasticity of an intact sensory projection after injury and ChABC treatment, we also looked at the response of primary afferents below the spinal injury level. CGRP immunostaining in spinal segment C5 revealed a normal expression pattern in control (uninjured) animals, with CGRP immunoreactivity present in primary afferent terminals in the superficial laminas of the dorsal horn, apparent as a thick band in lamina IIo with a smaller number of fibers terminating in the deep dorsal horn (Fig. 5*A*). A small proportion of CGRP-immunoreactive fibers were also present at the interface between the gracile and cuneate fasciculi in the dorsal columns (the fasciculus interfascicularis). A similar pattern of staining was seen in uninjured animals treated with ChABC (Fig. 5*B*). Four weeks after a C4 dorsal column lesion and vehicle treatment, CGRP immunoreactivity in the spinal segment below the injury (C5) was similar to that observed in control animals (Fig. 5*C*,*F*). However, after a C4 dorsal column lesion and ChABC treatment, CGRP immunoreactivity was present in aberrant locations in the spinal cord, most notably in the white matter of the degenerating dorsal columns where these fibers are not normally observed (Fig. 5*D*,*E*,*G*). Numerous CGRP-immunoreactive fibers were observed within the gracile fasciculus (Fig. 5*G*) and in superficial regions of the cuneate fasciculus, dorsal to their normal terminal regions in the dorsal horn (Fig. 5*E*). Aberrant primary afferent sprouting was only observed at spinal levels close to the injury site, within the C5 spinal segment. At sites more distal to the SCI, there was no evidence of aberrant primary afferent sprouting after injury and ChABC treatment; in more caudal cervical segments (C6–C8) and at more distal sites in the lumbar cord (L1–L3), the pattern of CGRP expression was similar to that of controls (data not shown). Quantification of CGRP immunoreactivity in the dorsal spinal cord one segment below the spinal injury (C5) confirmed the presence of enhanced CGRP immunoreactivity in aberrant areas of the dorsal columns after injury and treatment with ChABC (Fig. 5*H*). Measurements in four defined regions revealed that CGRP staining intensity had significantly increased compared with unlesioned controls (both naive and ChABC treated) in the gracile fasciculus and in medial, mediolateral, and lateral areas of the cuneate fasciculus (all $p < 0.05$, one-way ANOVA, Holm-Sidak *post hoc*). In lesioned animals treated with vehicle, there were no significant differences in CGRP staining intensities in

any of the defined regions from that of controls (all $p > 0.05$, one-way ANOVA, Holm-Sidak *post hoc*). Statistical comparisons of ChABC treatment compared with vehicle treatment after lesion also revealed a significant difference in the gracile, medial, and lateral areas ($p < 0.05$, one-way ANOVA, Holm-Sidak *post hoc*). Thus, treatment with ChABC induces sprouting of intact primary afferent projections caudal to an SCI, in areas of degenerating white matter.

Sprouting occurs in areas of CSPG degradation after SCI

To determine whether plasticity was specific to areas where ChABC treatment had effectively degraded CSPGs, the expression of C-4-S was determined using an antibody to the stub epitope, which remains after removal of GAG chains from CSPG molecules. In the cervical cord of sham (uninjured) controls and lesioned animals treated with vehicle, no immunoreactivity for C-4-S was detected at any level (Fig. 6*A*,*C*). In the cervical cord of uninjured animals treated with ChABC, intense C-4-S immunoreactivity was observed in spinal cord white matter, in dorsal, lateral, and ventral columns, with the greatest degree of CSPG degradation apparent in the gracile fasciculus (Fig. 6*B*). In lesioned animals treated with ChABC, intense C-4-S immunoreactivity was observed surrounding the lesion border, as observed previously (Lemons et al., 1999; Bradbury et al., 2002). However, in transverse sections of the spinal cord one segment above and below the SCI, the pattern of C-4-S immunoreactivity was similar to that of unlesioned animals treated with ChABC (Fig. 6, compare *B*, *D*). Thus, the intense immunoreactivity for chondroitin sulfate stub epitopes in the gracile fasciculus, dorsal portions of cuneate fasciculus, and ventral fasciculus confirmed that these areas were rich in CSPGs and that the GAG portion had been degraded by the intrathecal delivery of ChABC. However, in all of these areas, aberrant sprouting was observed after SCI plus ChABC, but not after ChABC treatment alone, implying that denervation may be required in addition to CSPG degradation for sprouting to occur. This was further investigated in colocalization experiments in which double staining for C-4-S and CGRP revealed that although there was an equivalent degree of CSPG digestion observed in ChABC-treated lesioned and unlesioned animals, primary afferent sprouting only occurred in the lesioned animals, where numerous CGRP-immunoreactive fibers were observed sprouting toward and within areas of CSPG degradation (Fig. 6, compare *F*, *H*). No positive staining for either C-4-S or CGRP was observed in the gracile fasciculus of sham (uninjured) controls or lesioned animals treated with vehicle (Fig. 6*E*,*G*). Thus, we find that CSPG degradation promotes sprouting within the spinal cord only after a denervation injury.

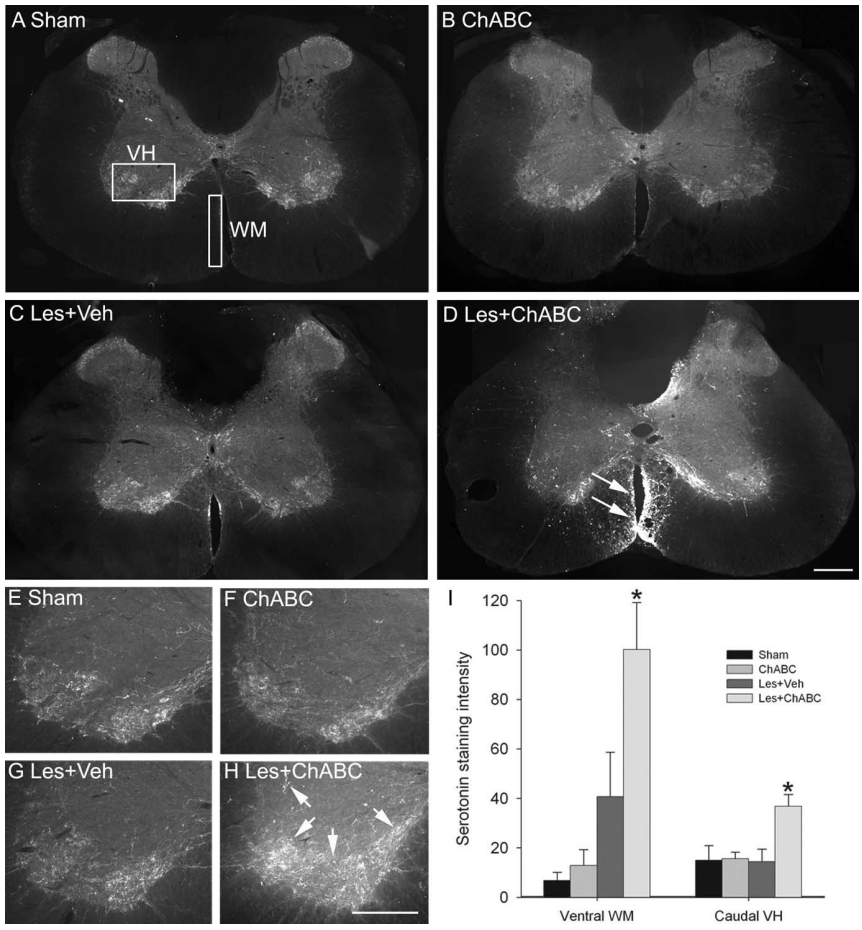

Figure 4. ChABC promotes plasticity of serotonergic fibers ventral and caudal to a C4 dorsal column lesion. ***A***, ***B***, Serotonin immunostaining in transverse sections of C4 spinal cord reveals serotonergic immunoreactivity to be expressed predominantly within the superficial dorsal horn, lamina X, and the ventral horn, with a similar pattern of expression observed in sham (unlesioned) animals (***A***) and ChABC-treated unlesioned animals (***B***). The boxed areas in ***A*** denote regions selected for quantification. ***C***, After dorsal column lesion and vehicle treatment, serotonergic immunoreactivity is similar to that of controls, with a slight increase observed in the ventral white matter adjacent to the ventral sulcus. ***D***, However, after dorsal column lesion and ChABC treatment, there is abundant sprouting of descending serotonergic fibers ventral to the lesion, with numerous intensely stained fibers apparent in ventral white matter (arrows). ***E–G***, Serotonergic innervation caudal to the lesion, within the C6 ventral horn, reveals a similar pattern of innervation in sham (unlesioned) animals (***E***), ChABC-treated unlesioned animals (***F***), and lesioned animals treated with vehicle (***G***). ***H***, In contrast, abundant serotonergic innervation of C6 ventral horn can be observed in lesioned animals treated with ChABC, with dense innervation of serotonergic terminal regions apparent (arrows). ***I***, Quantification confirmed a significant increase in serotonergic immunoreactivity in the ventral white matter at C4 and caudal ventral horn at C6 after ChABC but not vehicle treatment. Asterisks denote a significant difference from sham controls. Error bars indicate SEM. Scale bars, 200 μm. VH, Ventral horn; WM, white matter; Les, lesion; Veh, vehicle.

ChABC treatment does not lead to enhanced pain after SCI

Aberrant sprouting of primary afferents could have the potential detrimental effect of increasing nociceptive function, leading to an abnormal sensitivity to painful stimuli. Therefore, we investigated whether treatment with ChABC after SCI would result in an enhanced pain state. We performed these experiments at the lumbar spinal cord level because this is the most appropriate region for determining pain sensitivity in the hindpaw, which is a classical paradigm used in studies of pain and more established than pain studies in the forepaw. Over 4 weeks of postinjury testing, there was no development of thermal hyperalgesia to noxious heat stimuli applied to the hindpaws after a lumbar dorsal column lesion (level L2) and treatment with either vehicle or ChABC compared with sham controls ($p > 0.05$, two-way repeated-measures ANOVA) (Fig. 7*A*,*B*). Similarly, there was no development of mechanical allodynia in response to mechanical

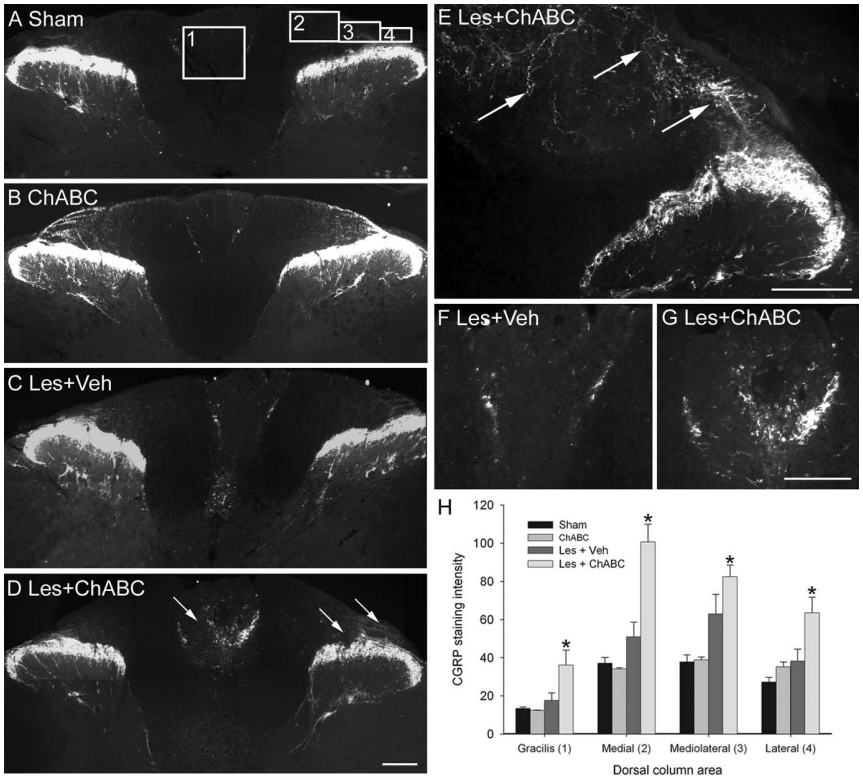

Figure 5. ChABC promotes plasticity of primary afferents caudal to a C4 dorsal column lesion. ***A***, ***B***, CGRP immunostaining in transverse sections of the cervical spinal cord at spinal level C5 reveals the normal pattern of primary afferent terminals in the superficial dorsal horn of sham (unlesioned) animals (***A***) and ChABC-treated unlesioned animals (***B***). The boxed areas in ***A*** denote regions selected for quantification. ***C***, ***F***, After a C4 dorsal column lesion and vehicle treatment, the pattern of CGRP immunoreactivity at level C5 was similar to that of controls. ***D***, ***E***, ***G***, However, in lesioned animals treated with ChABC, primary afferent sprouting was abundant, particularly in the degenerating dorsal columns, with numerous CGRP-immunoreactive fibers apparent within the gracile fasciculus and in superficial regions of the cuneate fasciculus, where these fibers are not normally present (arrows depict sprouting CGRP-immunoreactive fibers). ***H***, Quantification in four defined regions confirmed a significant increase in CGRP immunoreactivity in the gracile fasciculus and in medial, mediolateral, and lateral areas of the cuneate fasciculus after ChABC but not vehicle treatment. Asterisks denote a significant difference from sham controls. Error bars indicate SEM. Scale bars, 200 μm. Les, Lesion; Veh, vehicle.

stimulation applied to the hindpaws following this lesion and treatment with either vehicle or ChABC, compared with sham controls ($p > 0.05$, two-way repeated measures ANOVA; Fig. 7*C* and D). Thus, treatment with ChABC following dorsal column injury does not lead to increased pain sensitivity.

ChABC treatment does not result in increased functional connections onto spinal nociceptive neurons after SCI

To determine whether sprouting primary afferents lead to increased postsynaptic connections, we examined the expression of the immediate-early gene c-*fos* in the lumbar spinal cord after noxious heat stimulation of the hindpaw. In sham (unlesioned) animals, noxious heat induced the expression of c-*fos* in the L4/5 lumbar dorsal horn, with c-*fos* immunoreactivity apparent in the nuclei of neurons localized in laminas I and II (Fig. 8*A*,*B*). Five weeks after an L2 dorsal column lesion and treatment with either vehicle or ChABC, the expression of c-*fos* in L4/5 lumbar dorsal horn after noxious heat stimulation remained unchanged, with a similar pattern of c-*fos* immunoreactivity to that of controls (Fig. 8*C*–*F*). Quantification of the number of c-*fos*-immunoreactive cells in the dorsal horn at spinal levels L3–L6 confirmed that injury and treatment with ChABC did not result in any increased c-*fos* induction (Fig. 8*H*). In sham animals, the number of c-*fos*-immunoreactive nuclei was maximal in lumbar regions L4 and L5 with ~40 positive cells (±5.1), with a lower expression at levels L3 (~20 ± 1.4) and L6 (~7 ± 0.4). These values did not significantly differ after dorsal column lesion and treatment with either vehicle or ChABC (both $p > 0.05$, one-way ANOVA). In all cases, c-*fos* immunoreactivity was not apparent in the contralateral dorsal horn (data not shown). Thus, treatment with ChABC after SCI does not lead to increased functional connectivity of nociceptive neurons. To confirm that primary afferent sprouting had occurred at the lumbar level after L2 dorsal column lesion and ChABC treatment, adjacent sections were immunostained for CGRP. The expression of CGRP closely followed the pattern observed in cervical spinal cord, being expressed exclusively in primary afferent terminals in the dorsal horn in uninjured controls, with a similar expression observed in vehicle-treated lesioned animals (data not shown). However, as observed in the cervical cord, robust sprouting of primary afferents occurred in aberrant areas of the dorsal columns, with numerous sprouting CGRP-immunoreactive fibers present across the gracile fasciculus (Fig. 8*G*), an effect that was maximal within one segment of the injury.

Discussion

Here, we demonstrate that degrading CSPGs after SCI can promote sprouting of intact and injured spinal projections within the spinal cord. Treatment with ChABC induced plasticity of corticospinal, serotonergic, and primary afferent fibers in degenerating and denervated regions. No sprouting was observed in injured animals treated with vehicle or uninjured animals treated with ChABC. We also examined possible detrimental effects of sprouting but found no increase in pain sensitivity or connectivity of nociceptive neurons. This is the first demonstration that ChABC can induce plasticity within the spinal cord after SCI and suggests compensatory sprouting of descending projections as a mechanism underlying functional recovery.

Plasticity of descending systems

CST sprouting rostral to the lesion (determined by analyzing the dorsal column projection using PKCγ) occurred in dorsal regions of the dorsal columns, where this tract does not normally project. Because these fibers were in aberrant locations and in a region where CSPG degradation above the lesion is maximal, this is strong evidence that CSPG digestion promotes plasticity. Furthermore, at and caudal to the lesion level, numerous BDA-labeled fibers were observed in spinal gray matter, suggesting that ChABC-mediated sprouting leads to increased innervation of CST terminal regions and confirming previous observations that ChABC promotes frank regeneration of CST axons caudal to an SCI (Bradbury et al., 2002). In both rats and humans, a significant degree of functional improvement is known to occur spontaneously after

SCI. CST plasticity has been shown to contribute to this process via the formation of new circuits through collateral sprouting (Weidner et al., 2001; Bareyre et al., 2004; Raineteau and Schwab, 2001). Thus, a likely mechanism for the increased recovery observed after ChABC treatment is that degrading CSPGs enhances spontaneous CST plasticity, leading to increased innervation and connectivity within spinal gray matter. Similar observations have been made after neutralization of inhibitory CNS myelin components, where CST sprouting was associated with a recovery in locomotor function (Li and Strittmatter, 2003; Li et al., 2004, 2005). Other studies have demonstrated sprouting of the intact contralateral CST after unilateral pyramidotomy and anti-Nogo treatment strategies (Raineteau et al., 1999), which was also accompanied by recovery of forelimb motor behaviors (Thallmair et al., 1998; Z'Graggen et al., 1998).

We also observed sprouting of the intact descending raphe-spinal serotonergic system after SCI and ChABC treatment. Sprouting serotonergic fibers were observed ventral to the dorsal column injury at the injury level, in a zone of degeneration and CSPG degradation, and increased serotonin innervation in the ventral horn also occurred caudal to the injury. Spinal serotonin levels are known to facilitate locomotor function and may influence functional recovery after SCI (Saruhashi et al., 1996; Schmidt and Jordan, 2000). Furthermore, increased innervation of the ventral horn by sprouting serotonergic fibers after anti-Nogo treatments has been associated with a recovery in locomotor function (Bregman et al., 1995; Li and Strittmatter, 2003; Li et al., 2004, 2005). Thus, the serotonergic sprouting observed in the current study may be an additional mechanism underlying recovery of function after SCI and ChABC treatment.

These findings suggest that, similar to inhibitory factors associated with CNS myelin, CSPGs play a role in suppressing sprouting responses of injured and intact descending systems after injury. Because myelin inhibitors are highly expressed in degenerating white-matter tracts (Schwab and Bartholdi, 1996), the presence of these may have limited the extent of ChABC-induced sprouting in the white matter, which was only observed proximal to the injury (within one to two segments). In contrast, increased innervation in denervated gray matter (where myelin inhibitors are not highly expressed) occurred at more distal sites. Thus, targeting both myelin and CSPGs may be a future strategy for maximizing the potential for plasticity after SCI.

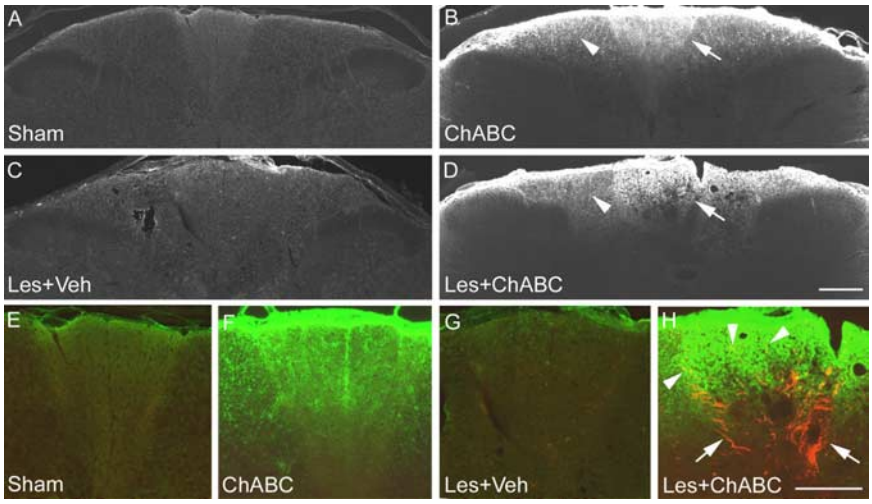

Figure 6. Sprouting occurs in areas of CSPG digestion after SCI. ***A***, ***C***, In C5 transverse sections, immunostaining for the C-4-S epitope (which is only present after successful digestion of CSPG GAGs) reveals no positive immunoreactivity in sham (uninjured) controls (***A***) and lesioned animals treated with vehicle (***C***). ***B***, ***D***, In unlesioned (***B***) and lesioned (***D***) animals treated with ChABC, intense C-4-S immunoreactivity is apparent in the dorsal columns, localized in superficial regions of the cuneate fasciculus (arrowheads) and in the gracile fasciculus (arrows), where immunoreactivity was particularly intense (an almost identical pattern was observed in C4 segments; data not shown). ***E***, ***G***, Colocalization of C-4-S (green) and CGRP (red) in high-power images of the graciile fasciculus show no positive staining in sham (uninjured) controls (***E***) and lesioned animals treated with vehicle (***G***). ***F***, ***H***, However, although the degree of CSPG digestion in unlesioned (***F***) and lesioned (***H***) animals treated with ChABC is comparable, primary afferent sprouting only occurs in the lesioned animals, with numerous CGRP-positive fibers apparent sprouting toward and within areas of CSPG digestion (***H***, arrows). Scale bars, 200 μm. Les, Lesion; Veh, vehicle.

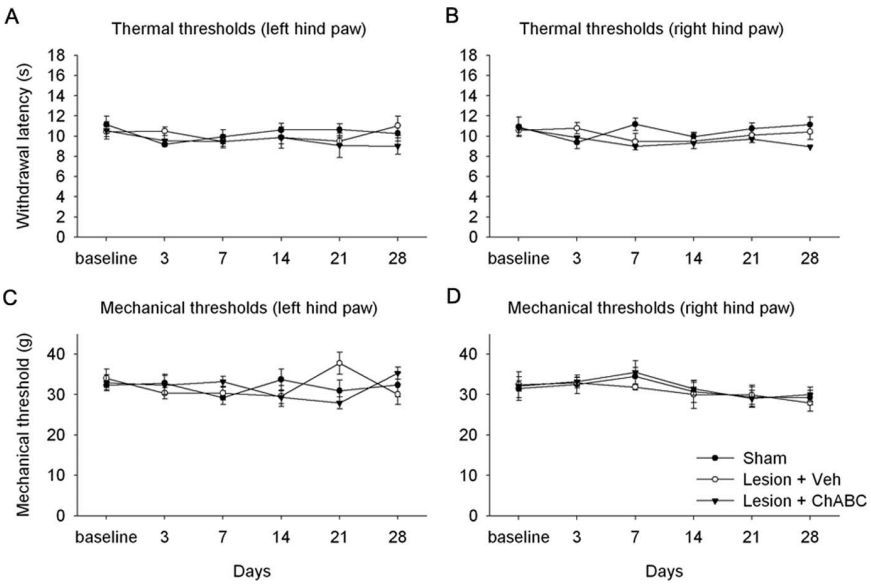

Figure 7. ChABC treatment does not lead to enhanced pain sensitivity after lumbar (L2) dorsal column injury. Group mean latencies for thermal (***A***, ***B***) or mechanical (***C***, ***D***) withdrawal thresholds over a 4 week postinjury testing period revealed that there was no development of thermal hyperalgesia or mechanical allodynia after dorsal column lesion and treatment with either vehicle (Veh) or ChABC. Thus, enhanced primary afferent sprouting after injury and ChABC treatment does not result in an increased sensitivity to pain. Error bars indicate SEM.

Primary afferent plasticity

We found that ChABC treatment promoted aberrant sprouting of CGRP-immunoreactive fibers below the level of an SCI, predominantly in regions of CSPG degradation in the degenerating dorsal columns. Primary afferent sprouting is typically associated with enhanced pain states (McMahon et al., 1995; Bennett et al., 2000; Romero et al., 2000) or conditions such as autonomic dysreflexia (Krenz et al., 1999; Weaver et al., 2001). However, despite robust primary afferent sprouting in lesioned animals treated

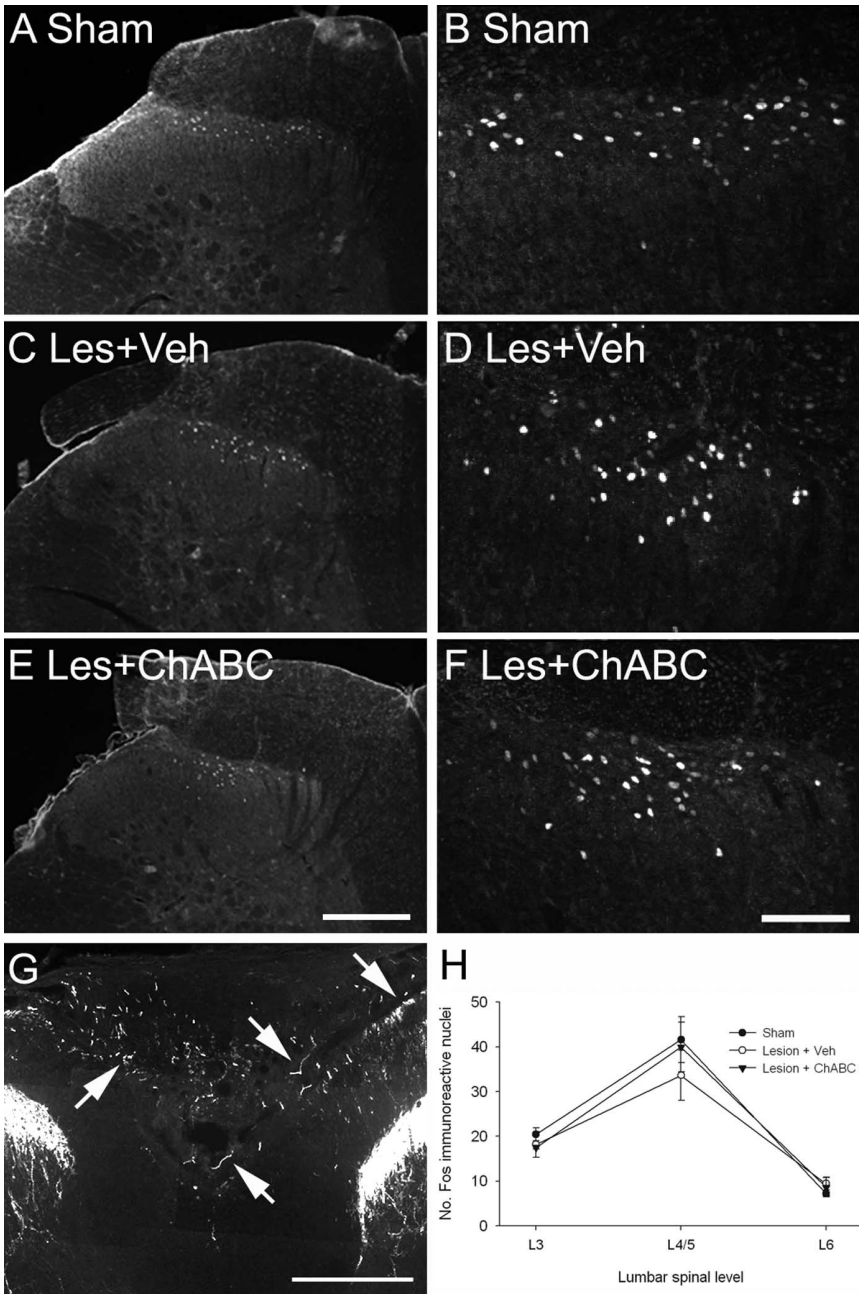

Figure 8. ChABC treatment does not lead to increased connectivity of nociceptive neurons after lumbar (L2) dorsal column injury. Transverse sections through the lumbar spinal cord (level L4/5) show c-*fos* expression in the dorsal horn 2 h after application of a noxious heat stimulus to the left hindpaw. ***A***, ***B***, In sham controls, noxious heat resulted in the induction of the immediate-early gene c-*fos*, with c-*fos*-immunoreactive nuclei apparent in the superficial laminas of the dorsal horn (***A***; shown in high power in ***B***). ***C–F***, After dorsal column injury and treatment with either vehicle (***C***, ***D***) or ChABC (***E***, ***F***), c-*fos* expression remained unchanged, with a similar pattern of expression to that of controls. ***G***, CGRP immunoreactivity in the lumbar cord of a lesioned animal treated with ChABC reveals that, similar to the observations in the cervical cord, primary afferent sprouting also occurred below the level of a lumbar dorsal column injury. ***H***, Cell counts at lumbar spinal levels L3–L6 confirmed that there were no significant differences in the number of c-*fos*-immunoreactive nuclei between groups, with c-*fos* expression maximal at levels L4/5 and fewer c-*fos*-immunoreactive nuclei apparent in L3 and L6 in all cases. Scale bars: ***A***, ***C***, ***E***, ***G***, 200 μm; ***B***, ***D***, ***F***, 100 μm. Les, Lesion; Veh, vehicle. Error bars indicate SEM.

with ChABC in the current study, no decrease in either mechanical or thermal pain thresholds or increased c-*fos* induction after noxious stimulation was observed. This could be explained by the location of the primary afferent sprouting, which was predominantly observed in the dorsal white matter rather than in the normal terminal regions in the dorsal horn. It is possible that any increased sprouting in the dorsal horn could have been masked by the high constitutive expression of CGRP in this region and, although the c-*fos* data suggest that there was no increased input to dorsal horn nociceptive neurons, this does not rule out increased connectivity with other target cells. One possible target for these sprouting afferents is the network of neurons located along the midline of the dorsal columns (Abbadie et al., 1999). Beneficial effects of primary afferent plasticity below an SCI have been reported previously (Goldberger and Murray, 1988; Helgren and Goldberger, 1993), with the recovery of postural reflexes and locomotion in hemisected cats being attributed to a compensatory increase in dorsal root projections to the partially denervated spinal cord. It is possible that degrading CSPGs promotes recovery via a similar mechanism, with enhanced afferent control contributing to behavioral changes. However, it is also possible that the sprouting primary afferents observed in the present study do not make any functional connections and so do not have any physiological effect. If this is the case, then this finding still stands as a robust demonstration that sprouting of intact systems can be induced after SCI and CSPG degradation and highlights the potential for this treatment to promote plasticity.

Factors governing ChABC-mediated plasticity

Previous studies have demonstrated ChABC-mediated plasticity in adult brain systems, but the rules governing such plasticity remain undetermined. For example, whether denervation is required has not previously been fully addressed. Plasticity observed after monocular deprivation (Pizzorusso et al., 2002) or denervation of the superior colliculus (Tropea et al., 2003) suggests that denervation or a similar challenge to the normal system is required. However, Purkinje axon sprouting has been observed in the uninjured cerebellum after ChABC treatment, although this was a transient effect (Corvetti and Rossi, 2005). In a recent study, functional plasticity was demonstrated in brainstem nuclei after SCI and ChABC treatment (Massey et al., 2006), but it was not determined whether ChABC alone could account for this plasticity. In the current study, we establish that ChABC treatment in the absence of injury does not induce plasticity in any of the three spinal systems studied, even though the pattern of CSPG degradation at rostral and caudal spinal levels was comparable to that of ChABC-treated lesioned animals. These results suggest that in the spinal cord the presence of both denervation and CSPG degradation is required for ChABC-induced sprouting to occur and

that unknown factors associated with degeneration lead to a sprouting response in spinal systems that is normally restricted by CSPGs. CSPG degradation unmasks this response and thus allows plasticity in these systems. Furthermore, our findings that sprouting of serotonergic and CST projections led to increased innervation of gray matter, whereas primary afferent sprouting did not, suggests that different systems have different propensities for sprouting, similar to the observations made in previous studies after dorsal rhizotomy injury (Goldberger and Murray, 1982).

Consequences of sprouting after SCI

Injury-induced sprouting is known to be more extensive in developing animals than in mature animals, accounting for their far greater capacity for recovery after CNS injury (Bernstein and Stelzner, 1983; Kapfhammer, 1997; Z'Graggen et al., 2000). Attempts to mimic this favorable sprouting in the injured adult CNS have become an increasing focus in SCI research. However, as well as beneficial effects (Thallmair et al., 1998; Raineteau and Schwab, 2001), increased sprouting could also have detrimental consequences (Romero et al., 2000; Weaver et al., 2006). Targeted treatments aimed at minimizing detrimental sprouting and optimizing beneficial sprouting will be a future goal for the treatment of spinal-injured patients. Indeed, the importance of balancing potentially opposing influences was highlighted in a recent study in which the beneficial effects on motor function observed after neural stem cell transplants were found to be limited by the development of allodynia, which was associated with aberrant sprouting (Hofstetter et al., 2005).

In the current study, we used the same injury model and treatment paradigm that has been shown previously to promote functional recovery after SCI (Bradbury et al., 2002) and have demonstrated that ChABC treatment induces significant plasticity of both intact and injured systems with no adverse effects on pain sensitivity. Such plasticity is likely to be one of the key mechanisms by which ChABC treatment promotes functional recovery after SCI. Additional understanding of the molecular mechanisms that govern plasticity will be an important step toward developing therapies aimed at optimizing the function of intact systems after spinal injury.

References

Abbadie C, Skinner K, Mitrovic I, Basbaum AI (1999) Neurons in the dorsal column white matter of the spinal cord: complex neuropil in an unexpected location. Proc Natl Acad Sci USA 96:260–265.

Asher RA, Morgenstern DA, Fidler PS, Adcock KH, Oohira A, Braistead JE, Levine JM, Margolis RU, Rogers JH, Fawcett JW (2000) Neurocan is upregulated in injured brain and in cytokine-treated astrocytes. J Neurosci 20:2427–2438.

Asher RA, Morgenstern DA, Shearer MC, Adcock KH, Pesheva P, Fawcett JW (2002) Versican is upregulated in CNS injury and is a product of oligodendrocyte lineage cells. J Neurosci 22:2225–2236.

Bareyre FM, Kerschensteiner M, Raineteau O, Mettenleiter TC, Weinmann O, Schwab ME (2004) The injured spinal cord spontaneously forms a new intraspinal circuit in adult rats. Nat Neurosci 7:269–277.

Bennett AD, Chastain KM, Hulsebosch CE (2000) Alleviation of mechanical and thermal allodynia by CGRP(8-37) in a rodent model of chronic central pain. Pain 86:163–175.

Bernstein DR, Stelzner DJ (1983) Plasticity of the corticospinal tract following midthoracic spinal injury in the postnatal rat. J Comp Neurol 221:382–400.

Bradbury EJ, McMahon SB (2006) Spinal cord repair strategies: why do they work? Nat Rev Neurosci 7:644–653.

Bradbury EJ, Moon LD, Popat RJ, King VR, Bennett GS, Patel PN, Fawcett JW, McMahon SB (2002) Chondroitinase ABC promotes functional recovery after spinal cord injury. Nature 416:636–640.

Bregman BS, Kunkel-Bagden E, Schnell L, Dai HN, Gao D, Schwab ME (1995) Recovery from spinal cord injury mediated by antibodies to neurite growth inhibitors. Nature 378:498–501.

Bruce JC, Oatway MA, Weaver LC (2002) Chronic pain after clip-compression injury of the rat spinal cord. Exp Neurol 178:33–48.

Caggiano AO, Zimber MP, Ganguly A, Blight AR, Gruskin EA (2005) Chondroitinase ABCI improves locomotion and bladder function following contusion injury of the rat spinal cord. J Neurotrauma 22:226–239.

Carulli D, Laabs T, Geller HM, Fawcett JW (2005) Chondroitin sulfate proteoglycans in neural development and regeneration. Curr Opin Neurobiol 15:116–120.

Chau CH, Shum DK, Li H, Pei J, Lui YY, Wirthlin L, Chan YS, Xu XM (2004) Chondroitinase ABC enhances axonal regrowth through Schwann cell-seeded guidance channels after spinal cord injury. FASEB J 18:194–196.

Corvetti L, Rossi F (2005) Degradation of chondroitin sulfate proteoglycans induces sprouting of intact Purkinje axons in the cerebellum of the adult rat. J Neurosci 25:7150–7158.

Davies SJ, Fitch MT, Memberg SP, Hall AK, Raisman G, Silver J (1997) Regeneration of adult axons in white matter tracts of the central nervous system. Nature 390:680–683.

Davies SJ, Goucher DR, Doller C, Silver J (1999) Robust regeneration of adult sensory axons in degenerating white matter of the adult rat spinal cord. J Neurosci 19:5810–5822.

De Winter F, Holtmaat AJ, Verhaagen J (2002) Neuropilin and class 3 semaphorins in nervous system regeneration. Adv Exp Med Biol 515:115–139.

Dou CL, Levine JM (1994) Inhibition of neurite growth by the NG2 chondroitin sulfate proteoglycan. J Neurosci 14:7616–7628.

Dou CL, Levine JM (1997) Identification of a neuronal cell surface receptor for a growth inhibitory chondroitin sulfate proteoglycan (NG2). J Neurochem 68:1021–1030.

Filbin MT (2003) Myelin-associated inhibitors of axonal regeneration in the adult mammalian CNS. Nat Rev Neurosci 4:703–713.

Fouad K, Schnell L, Bunge MB, Schwab ME, Liebscher T, Pearse DD (2005) Combining Schwann cell bridges and olfactory-ensheathing glia grafts with chondroitinase promotes locomotor recovery after complete transection of the spinal cord. J Neurosci 25:1169–1178.

Goldberger ME, Murray M (1982) Lack of sprouting and its presence after lesions of the cat spinal cord. Brain Res 241:227–239.

Goldberger ME, Murray M (1988) Patterns of sprouting and implications for recovery of function. Adv Neurol 47:361–385.

Grimpe B, Pressman Y, Lupa MD, Horn KP, Bunge MB, Silver J (2005) The role of proteoglycans in Schwann cell/astrocyte interactions and in regeneration failure at PNS/CNS interfaces. Mol Cell Neurosci 28:18–29.

Hargreaves K, Dubner R, Brown F, Flores C, Joris J (1988) A new and sensitive method for measuring thermal nociception in cutaneous hyperalgesia. Pain 32:77–88.

Helgren ME, Goldberger ME (1993) The recovery of postural reflexes and locomotion following low thoracic hemisection in adult cats involves compensation by undamaged primary afferent pathways. Exp Neurol 123:17–34.

Hofstetter CP, Holmstrom NA, Lilja JA, Schweinhardt P, Hao J, Spenger C, Wiesenfeld-Hallin Z, Kurpad SN, Frisen J, Olson L (2005) Allodynia limits the usefulness of intraspinal neural stem cell grafts; directed differentiation improves outcome. Nat Neurosci 8:346–353.

Houle JD, Tom VJ, Mayes D, Wagoner G, Phillips N, Silver J (2006) Combining an autologous peripheral nervous system "bridge" and matrix modification by chondroitinase allows robust, functional regeneration beyond a hemisection lesion of the adult rat spinal cord. J Neurosci 26:7405–7415.

Ikegami T, Nakamura M, Yamane J, Katoh H, Okada S, Iwanami A, Watanabe K, Ishii K, Kato F, Fujita H, Takahashi T, Okano HJ, Toyama Y, Okano H (2005) Chondroitinase ABC combined with neural stem/progenitor cell transplantation enhances graft cell migration and outgrowth of growth-associated protein-43-positive fibers after rat spinal cord injury. Eur J Neurosci 22:3036–3046.

Jones LL, Margolis RU, Tuszynski MH (2003) The chondroitin sulfate proteoglycans neurocan, brevican, phosphacan, and versican are differentially regulated following spinal cord injury. Exp Neurol 182:399–411.

Kapfhammer JP (1997) Axon sprouting in the spinal cord: growth promoting and growth inhibitory mechanisms. Anat Embryol (Berl) 196:417–426.

Krenz NR, Meakin SO, Krassioukov AV, Weaver LC (1999) Neutralizing

intraspinal nerve growth factor blocks autonomic dysreflexia caused by spinal cord injury. J Neurosci 19:7405–7414.
Lemons ML, Howland DR, Anderson DK (1999) Chondroitin sulfate proteoglycan immunoreactivity increases following spinal cord injury and transplantation. Exp Neurol 160:51–65.
Li S, Strittmatter SM (2003) Delayed systemic Nogo-66 receptor antagonist promotes recovery from spinal cord injury. J Neurosci 23:4219–4227.
Li S, Liu BP, Budel S, Li M, Ji B, Walus L, Li W, Jirik A, Rabacchi S, Choi E, Worley D, Sah DW, Pepinsky B, Lee D, Relton J, Strittmatter SM (2004) Blockade of Nogo-66, myelin-associated glycoprotein, and oligodendrocyte myelin glycoprotein by soluble Nogo-66 receptor promotes axonal sprouting and recovery after spinal injury. J Neurosci 24:10511–10520.
Li S, Kim JE, Budel S, Hampton TG, Strittmatter SM (2005) Transgenic inhibition of Nogo-66 receptor function allows axonal sprouting and improved locomotion after spinal injury. Mol Cell Neurosci 29:26–39.
Massey JM, Hubscher CH, Wagoner MR, Decker JA, Amps J, Silver J, Onifer SM (2006) Chondroitinase ABC digestion of the perineuronal net promotes functional collateral sprouting in the cuneate nucleus after cervical spinal cord injury. J Neurosci 26:4406–4414.
McGee AW, Strittmatter SM (2003) The Nogo-66 receptor: focusing myelin inhibition of axon regeneration. Trends Neurosci 26:193–198.
McKeon RJ, Hoke A, Silver J (1995) Injury-induced proteoglycans inhibit the potential for laminin-mediated axon growth on astrocytic scars. Exp Neurol 136:32–43.
McMahon SB, Bennett DL, Priestley JV, Shelton DL (1995) The biological effects of endogenous nerve growth factor on adult sensory neurons revealed by a trkA-IgG fusion molecule. Nat Med 1:774–780.
Moon LD, Asher RA, Rhodes KE, Fawcett JW (2001) Regeneration of CNS axons back to their target following treatment of adult rat brain with chondroitinase ABC. Nat Neurosci 4:465–466.
Mori M, Kose A, Tsujino T, Tanaka C (1990) Immunocytochemical localization of protein kinase C subspecies in the rat spinal cord: light and electron microscopic study. J Comp Neurol 299:167–177.
Neafsey EJ, Hurley-Gius KM, Arvanitis D (1986) The topographical organization of neurons in the rat medial frontal, insular and olfactory cortex projecting to the solitary nucleus, olfactory bulb, periaqueductal gray and superior colliculus. Brain Res 377:561–570.
Neumann S, Woolf CJ (1999) Regeneration of dorsal column fibers into and beyond the lesion site following adult spinal cord injury. Neuron 23:83–91.
Pizzorusso T, Medini P, Berardi N, Chierzi S, Fawcett JW, Maffei L (2002) Reactivation of ocular dominance plasticity in the adult visual cortex. Science 298:1248–1251.
Raineteau O, Schwab ME (2001) Plasticity of motor systems after incomplete spinal cord injury. Nat Rev Neurosci 2:263–273.
Raineteau O, Z'Graggen WJ, Thallmair M, Schwab ME (1999) Sprouting and regeneration after pyramidotomy and blockade of the myelin-associated neurite growth inhibitors NI 35/250 in adult rats. Eur J Neurosci 11:1486–1490.
Rhodes KE, Fawcett JW (2004) Chondroitin sulphate proteoglycans: preventing plasticity or protecting the CNS? J Anat 204:33–48.
Romero MI, Rangappa N, Li L, Lightfoot E, Garry MG, Smith GM (2000) Extensive sprouting of sensory afferents and hyperalgesia induced by conditional expression of nerve growth factor in the adult spinal cord. J Neurosci 20:4435–4445.
Saruhashi Y, Young W, Perkins R (1996) The recovery of 5-HT immunoreactivity in lumbosacral spinal cord and locomotor function after thoracic hemisection. Exp Neurol 139:203–213.
Schmidt BJ, Jordan LM (2000) The role of serotonin in reflex modulation and locomotor rhythm production in the mammalian spinal cord. Brain Res Bull 53:689–710.
Schwab ME (2004) Nogo and axon regeneration. Curr Opin Neurobiol 14:118–124.
Schwab ME, Bartholdi D (1996) Degeneration and regeneration of axons in the lesioned spinal cord. Physiol Rev 76:319–370.
Silver J, Miller JH (2004) Regeneration beyond the glial scar. Nat Rev Neurosci 5:146–156.
Smith-Thomas LC, Fok-Seang J, Stevens J, Du JS, Muir E, Faissner A, Geller HM, Rogers JH, Fawcett JW (1994) An inhibitor of neurite outgrowth produced by astrocytes. J Cell Sci 107:1687–1695.
Smith-Thomas LC, Stevens J, Fok-Seang J, Faissner A, Rogers JH, Fawcett JW (1995) Increased axon regeneration in astrocytes grown in the presence of proteoglycan synthesis inhibitors. J Cell Sci 108:1307–1315.
Snow DM, Lemmon V, Carrino DA, Caplan AI, Silver J (1990) Sulfated proteoglycans in astroglial barriers inhibit neurite outgrowth in vitro. Exp Neurol 109:111–130.
Tang X, Davies JE, Davies SJ (2003) Changes in distribution, cell associations, and protein expression levels of NG2, neurocan, phosphacan, brevican, versican V2, and tenascin-C during acute to chronic maturation of spinal cord scar tissue. J Neurosci Res 71:427–444.
Thallmair M, Metz GA, Z'Graggen WJ, Raineteau O, Kartje GL, Schwab ME (1998) Neurite growth inhibitors restrict plasticity and functional recovery following corticospinal tract lesions. Nat Neurosci 1:124–131.
Tropea D, Caleo M, Maffei L (2003) Synergistic effects of brain-derived neurotrophic factor and chondroitinase ABC on retinal fiber sprouting after denervation of the superior colliculus in adult rats. J Neurosci 23:7034–7044.
Weaver LC, Verghese P, Bruce JC, Fehlings MG, Krenz NR, Marsh DR (2001) Autonomic dysreflexia and primary afferent sprouting after clip-compression injury of the rat spinal cord. J Neurotrauma 18:1107–1119.
Weaver LC, Marsh DR, Gris D, Brown A, Dekaban GA (2006) Autonomic dysreflexia after spinal cord injury: central mechanisms and strategies for prevention. Prog Brain Res 152:245–263.
Weidner N, Ner A, Salimi N, Tuszynski MH (2001) Spontaneous corticospinal axonal plasticity and functional recovery after adult central nervous system injury. Proc Natl Acad Sci USA 98:3513–3518.
Widenfalk J, Lundstromer K, Jubran M, Brene S, Olson L (2001) Neurotrophic factors and receptors in the immature and adult spinal cord after mechanical injury or kainic acid. J Neurosci 21:3457–3475.
Yick LW, Cheung PT, So KF, Wu W (2003) Axonal regeneration of Clarke's neurons beyond the spinal cord injury scar after treatment with chondroitinase ABC. Exp Neurol 182:160–168.
Yick LW, So KF, Cheung PT, Wu WT (2004) Lithium chloride reinforces the regeneration-promoting effect of chondroitinase ABC on rubrospinal neurons after spinal cord injury. J Neurotrauma 21:932–943.
Yu X, Bellamkonda RV (2001) Dorsal root ganglia neurite extension is inhibited by mechanical and chondroitin sulfate-rich interfaces. J Neurosci Res 66:303–310.
Z'Graggen WJ, Metz GA, Kartje GL, Thallmair M, Schwab ME (1998) Functional recovery and enhanced corticofugal plasticity after unilateral pyramidal tract lesion and blockade of myelin-associated neurite growth inhibitors in adult rats. J Neurosci 18:4744–4757.
Z'Graggen WJ, Fouad K, Raineteau O, Metz GA, Schwab ME, Kartje GL (2000) Compensatory sprouting and impulse rerouting after unilateral pyramidal tract lesion in neonatal rats. J Neurosci 20:6561–6569.
Zuo J, Neubauer D, Dyess K, Ferguson TA, Muir D (1998) Degradation of chondroitin sulfate proteoglycan enhances the neurite-promoting potential of spinal cord tissue. Exp Neurol 154:654–662. W